European Polymer Journal 45 (2009) 2564–2571

Contents lists available at ScienceDirect

European Polymer Journal

journal homepage: www.elsevier.com/locate/europolj

Macromolecular Nanotechnology

Photocontrol of supramolecular architecture in azopolymers: Achiral and chiral aggregation

Rosa M. Tejedor [a], Jose-Luis Serrano [b], Luis Oriol [a,*]

[a] Polymer and Liquid Crystal Group, Facultad de Ciencias-Instituto de Ciencia y Materiales de Aragón, Universidad de Zaragoza-CSIC, Pedro Cerbuna 12, E-50009 Zaragoza, Spain
[b] Polymer and Liquid Crystal Group, Instituto Universitario de Nanociencia de Aragón, Universidad de Zaragoza, Pedro Cerbuna 12, E-50009 Zaragoza, Spain

ARTICLE INFO

Article history:
Received 23 February 2009
Received in revised form 28 April 2009
Accepted 5 May 2009
Available online 12 May 2009

Keywords:
Azopolymers
Supramolecular chirality
Aggregates
Liquid crystal polymers

ABSTRACT

The absorption spectra and circular dichroism responses upon irradiation with 488 nm circularly polarized light (CPL) have been studied on polymeric films processed from two nematic copolymers containing azobenzene chromophores. Influence of the aggregation and orientation of azobenzenes on the photoinduced chiroptical properties has been analyzed. Moreover, polymeric films and 4 μm planar cells filled with the copolymers were studied by polarized optical microscopy (POM) with the aim of investigating the change of macroscopic optical properties and textures of azopolymers upon irradiation with CPL.

1. Introduction

The understanding and control of chirality is an important objective in life and materials science. In this case, the induction of chirality by physicochemical processes is an exciting opportunity for many scientists [1], particularly the generation of supramolecular chiral architectures. In these cases, a chiral physical force field, for example circularly polarized light [2], can be used to induce the initial asymmetry [3]. Thus, the asymmetry information is transferred by means of non-covalent interactions from a molecular to a supramolecular level [4].

The azobenzene unit exhibits fascinating photochemical behavior based on the *E*/*Z* photoisomerization, which has been widely investigated, and in particular the Weiger effect to induce optical properties such as birefringence and dichroism in azopolymers [5–8]. In addition, the relatively large structural change that occurs upon reversible isomerization influences the surrounding region. These units can act as mediators for processes that occur at the molecular level and can be transferred to a supramolecular level and, ultimately, to macroscopic phenomena. This transfer process is especially effective in liquid crystalline systems due to the cooperative interaction of mesogenic azobenzene units [9,10].

The irradiation of azobenzene units with chiral radiation (CPL) gives rise to very interesting results such as the induced reversible enantiodifferentiating photoisomerization of bicyclic azobenzene dimers [11]. In addition, enantiomeric excess values of two chiral domains in a Bx phase of bent-core molecules has been obtained using CPL [12]. Sierra and co-workers reported the induction of supramolecular chirality within the columnar mesophase of achiral mesogens [13]. In relation to polymeric materials [14], Nikolova et al. detected the photoinduction of a large circular birefringence and circular dichroism (CD) in films of a side-chain liquid crystalline azopolyester by illumination with CPL [15]. Similar effects were observed in amorphous polymers, but in these cases a pre-orientation was required [16] or irradiation with elliptically polarized light was used to induce supramolecular chirality in an amorphous azopolymer [17]. Cipparrone et al. described the photoinduction of supramolecular chiral structures by

---

* Corresponding author. Fax: +34 976762686.
E-mail address: loriol@unizar.es (L. Oriol).

0014-3057/$ - see front matter © 2009 Elsevier Ltd. All rights reserved.
doi:10.1016/j.eurpolymj.2009.05.010

CPL irradiation of an amorphous and achiral azopolymer without pre-alignment [18]. Natansohn et al. reported the photoinduction of a chiral supramolecular structure by illumination of a smectic azopolymer with CPL and the photoinduction of circular dichroism and birefringence in achiral copolymers with low contents of azobenzene units [19,20]. A circular Bragg reflection in the CD spectrum has been reported for a nematic azopolymer film irradiated with CPL [21]. The photofabrication of superhelix-like patterns [22,23] and other optical measurements demonstrated the photoinduction of a chiral arrangement in azopolymers [24,25]. Moreover, photoinduced supramolecular chirality was probed after irradiation with CPL of main-chain polymeric liquid crystal systems doped with azobenzene-containing W-shaped molecules [26]. Recently, we studied the thermal stability of the photoinduced supramolecular chiral organization in achiral homopolymer based on cyanoazobenzene [27] and the electronic and vibrational dichroism photoinduced in an achiral glassy nematic homopolymer containing metoxyazobenzenes as chromophores [28]. We present here a study of the control of the non-covalent interaction as a means to manage the supramolecular architecture of azobenzene units in side-chain nematic copolymers having both cyano and methoxyazobenzenes. CPL as a source of chiral information has been used in order to induce supramolecular chirality in these azopolymers. Self-assembly of chromophores in aggregates and its influence on chiroptical properties of polymeric films has been studied as well as the influence of irradiation on optical textures exhibited by these copolymers.

2. Experimental

2.1. Synthesis of materials

The monomers 4-methoxy-4′-(ω-methacryloyloxyhexyloxy) azobenzene and 4-cyano-4′-(ω-methacryloyloxyethyloxy) azobenzene were synthesized according to methods described previously [29]. P50 and P90 (Fig. 1) were prepared by a free radical chain polymerization. The synthesis of P50 is described as an example: 0.75 mmol of each monomer, 10 mL of freshly distilled dry DMF and 2.5 mol% AIBN were introduced into a Schlenck reactor. An inert atmosphere was achieved by several freeze-thaw cycles under vacuum and the introduction of argon to remove residual air. The reaction mixture was heated at 70 °C for 120 h, allowed to cool and poured into 250 mL of cold ethanol. The solid product was dissolved in chloroform, reprecipitated into methanol and the resulting polymer was extracted in a Soxhlet apparatus with ethanol for 48 h. The polymers were purified by flash column chromatography using silica gel (dichloromethane as eluant) and dried under vacuum at 50 °C to constant weight (determined by thermogravimetry). The final copolymer composition was determined from elemental analysis, FTIR spectra and ^{1}H NMR.

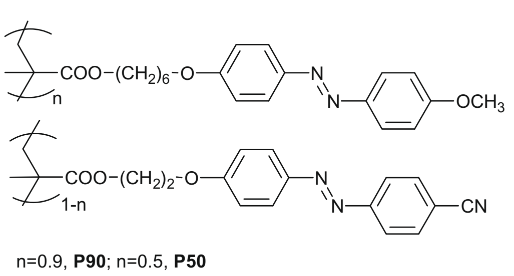

Fig. 1. Structure of the synthesized polymers: P50 and P90.

P50 (73%): Found: C, 69.13; H, 6.31; N, 8.90. ν/cm^{-1} (KBr) 2223 (CN), 1724 (C═O), 1247, 1141, 1025 (C–O), 838 (Ar). δ_H(400 Hz; CDCl$_3$; Me$_4$Si) 7.90–7.70 (m, aromatic), 7.70–7.57 (m, aromatic), 7.00–6.73 (m, aromatic), 4.41–4.00 (m, CH$_2$–O), 4.00–3.70 (m, CH$_2$–O, CH$_3$–O), 2.10–0.80 (m, CH$_2$, CH$_3$).

P90 (75%): Found: C, 69.57; H, 6.98; N, 7.50. ν/cm^{-1} (KBr) 2225 (CN), 1723 (C═O), 1246, 1143, 1026 (C–O), 838 (Ar). δ_H(400 Hz; CDCl$_3$; Me$_4$Si) 7.90–7.70 (m, aromatic), 7.70–7.57 (m, aromatic), 7.00–6.75 (m, aromatic), 4.40–4.00 (m, CH$_2$–O), 4.00–3.70 (m, CH$_2$–O, CH$_3$–O), 2.10–0.70 (m, CH$_2$, CH$_3$).

2.2. Material processing and irradiation

Thin films (thickness about 300 nm) were prepared by casting solutions of the polymers in chloroform onto clean, fused silica slides. The films were dried under vacuum at 30 °C during 24 h. The films were then heated above the clearing temperature (T_i) for 5 min and annealed for 15 min at 110 °C (nematic mesophase). The samples were then placed on a metal block at 25 °C for 30 min. This process gave rise to films that had a polydomain nematic glassy phase.

Annealed films of P50 and P90 were irradiated for 30 min with *left*-circularly polarized light (*l*-CPL) from the 488 nm line of an Ar$^+$ laser (power 20 mW/cm^2). UV–vis and CD spectra of all the illuminated films were recorded after keeping the samples in the dark at room temperature for 30 min. In order to evaluate the thermal stability of the photoinduced supramolecular order, illuminated polymeric films were successively annealed at different temperatures for 5 min and then cooled to room temperature. The CD spectrum was registered after each treatment.

Four micrometer cells with an aligning layer for planar orientation were filled with the copolymers in the isotropic state and slowly cooled down to room temperature. Thick films to POM studies were prepared by pressing a polymeric sample in the isotropic state and placed between two glass slides. Oriented planar cells and, also, thick samples were irradiated for 30 min with *l*-CPL from the 488 nm line of an Ar$^+$ laser (power 20 mW/cm^2) and studied by POM before and after irradiation.

2.3. Techniques

Elemental analyses were performed using a Perkin–Elmer 2400 Series II analyzer. FTIR spectra were registered using a Nicolet Avatar 380 spectrophotometer using KBr pellets. NMR spectra were registered using a Bruker AV-4 400 MHz spectrometer using CDCl$_3$ as solvent. Molecular weights and polydispersities were measured by GPC using a Waters 600E HPLC (Waters Styragel columns HR2 and HR4) with a

Table 1
Molecular weight, thermal stability, thermal transitions and mesomorphism determined by GPC, DSC, POM and X-ray diffraction for P50 and P90.

Polymer	M_n	M_w/M_n	T_{dec} (°C)[a]	T_{DGT} (°C)[b]	Thermal transition (°C)[c]
P50	13675	2.3	235	347/400	g 74 N 142 I
P90	18150	2.2	250	355/410	g 72 S 99 N 135 I

[a] T_{dec}: Onset of decomposition detected on the thermogravimetric curve.
[b] T_{DTG}: Temperature of maximum decomposition detected on the derivative thermogravimetric analysis.
[c] Measured by DSC on the second heating scan.

UV Waters 991 photodiode array detector. THF was used as the eluant and standard samples of polystyrene were employed. Thermal stability was measured by thermogravimetry using a TA Instruments STD 2960 apparatus at 10 °C/min under a nitrogen atmosphere. Thermal transitions were measured using a DSC-MDSC TA Instruments 2910 calorimeter at 10 °C/min under a nitrogen atmosphere. T_g values were measured as the midpoint in the heat capacity increase and the other transitions were taken as the maximum of the transition peak. Mesomorphism and modification of the optical textures were investigated using an Olympus BH-2 polarizing optical microscope (POM) equipped with a Linkam THMS-600 hot stage and a Linkam TMS91 temperature controller. UV–vis spectra were registered using a Unicam UV4-200 spectrophotometer or simultaneously with the CD spectrum using a Jasco J-810 Spectropolarimeter. CD was measured using a Jasco J-710 Spectropolarimeter or Jasco J-810 Spectropolarimeter. The films deposited onto fused silica slides were placed in a rotating holder around the light beam and CD spectra were registered every 60°. Film thickness was measured using a DEKTAK perfilometer. PeakFit v4.11 was used for the fitting procedure.

3. Results and discussion

3.1. Polymer properties

The molecular weight, polydispersity and thermal properties of the synthesized copolymers are collected in Table 1. ^{1}H NMR figures and details about copolymer composition determined by NMR are collected in Supplementary Information. These materials have good thermal stability and weight loss was not observed at temperatures below 230 °C. The mesomorphic properties of the synthesized polymers were determined by DSC, POM and X-ray diffraction. The mesomorphic properties of P90 are similar to those exhibited by the homopolymer bearing 4-methoxyazobenzene units [28] and shows a smectic phase above the T_g that undergoes a transition into a nematic melt before isotropization. However, copolymer P50, which has a high content of 4-cyanoazobenzene with a short flexible spacer, only exhibits a nematic phase over a broad temperature range.

3.2. Supramolecular arrangements of azobenzene units: UV–vis study

The UV–vis spectra of P50 and P90 were registered on as-prepared, annealed and irradiated thin films (Fig. 2 and Table 2). Moreover, UV–vis spectra of P50 and P90 were registered on THF solutions (see Fig S1 in Supplementary Information). In general, the UV–vis absorption spectra of the polymers containing methoxyazobenzene or cyanobenzene groups are characterized by a $\phi-\phi^*$ transition of aromatic rings at 250 nm, a strong $\pi-\pi^*$ transition between 340 and 365 nm and a weak n-π^* transitions at around 450 nm [30,31]. The bands at around 250 and 450 nm do not exhibit a significant dependence on the pretreatment of the polymeric film, but the $\pi-\pi^*$ transition is influenced by thermal annealing and irradiation as a consequence of the modification of the aggregation and the orientation of the chromophores [32]. The maximum of the absorption band due to the $\pi-\pi^*$ transition of *E*-azobenzene chromophores of both copolymers in THF solution was close to 360 nm (see Supplementary Information), whereas as-prepared cast films show broader and blue-shifted $\pi-\pi^*$ transition bands with a maximum at 345 nm. After

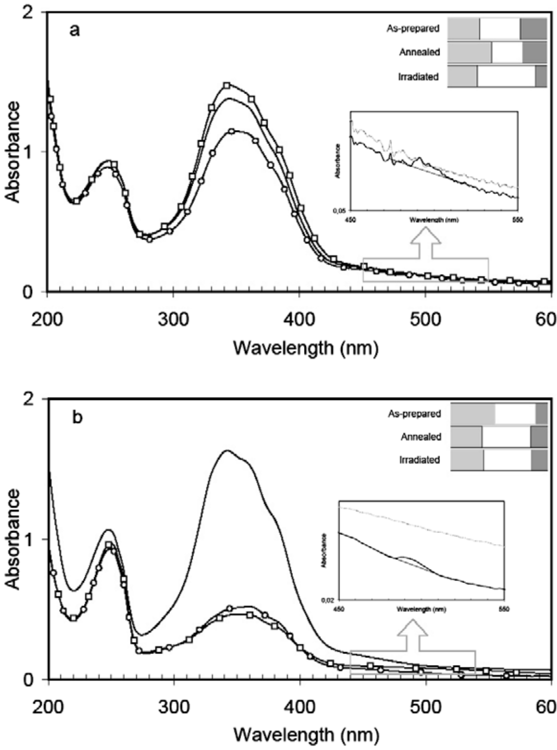

Fig. 2. UV–vis spectra of (a) P50 and (b) P90, as-prepared cast film (▬▬), annealed film (▬□▬) and film irradiated with *l*-CPL from the 488 nm line of an Ar$^+$ laser (20 mW/cm^2) for 30 min (▬○▬). Estimated percentage of the chromophores by fitting: H-aggregates (▨), free chromophores (□) and J-aggregates (■).

Table 2
UV–vis data corresponding to π–π^* transition bands of *E*-azobenzene units in THF solutions and thin films of the synthesized copolymers.

Sample	THF solution	Cast film	Annealed film	Irradiated film
P50				
λ_{max} (nm)	360	345	345	346
$A_{\pi-\pi^*}/A_{\Phi-\Phi^*}$	2.0	1.41	1.50	1.27
P90				
λ_{max} (nm)	360	345	356	360
$A_{\pi-\pi^*}/A_{\Phi-\Phi^*}$	2.0	1.43	0.48	0.57

annealing in the nematic phase and irradiation with *l*-CPL, the UV–vis spectrum of the studied polymeric films depends on the percentage of *p*-methoxyazobenzene moieties. The UV–vis spectrum of P50 after annealing retains the blue-shifted π–π^* band at about 345 nm, similar to the as-prepared cast film. After irradiation of the annealed film only a slight hypochromic effect of the main band at 345 nm is observed. However, the UV–vis spectrum of P90 after annealing is characterized by a λ_{max} (around 360 nm) similar to the THF solution but a noteworthy hypochromic effect is now detected. Moreover, the spectra of the P90 annealed films before and after irradiation are similar.

In solution, the absorption maxima of both copolymers are located at 360 nm and the narrow absorption bands indicate randomly oriented free azobenzene groups. In the solid state the azobenzene units in close proximity can associate with one another to form aggregates. Furthermore the thermal annealing can determine the aggregation fraction and the relationship between the type of aggregates [33,34], as well as the orientation of the chromophores. The contribution of associated and non-associated chromophores on the absorption bands of the copolymers P50 and P90 films was roughly estimated by using a peak fitting procedure. Good and reproducible fitting results were obtained by introducing three peaks with fixed absorption maxima at 334 nm for H-like aggregates, 360 nm for non-associated units and 384 nm for J-like aggregates of chromophores according to fitting procedure previously described [35–37]. Qualitative relationships between the chromophores in the different associated and non-associated arrangements were determined as the area of the corresponding peak and the results are compiled as percentages in Fig. 2. From the analysis of the fitting results it can be concluded that P50 shows an increase in aggregation after annealing and a decrease after irradiation. However, a reduction of the aggregation is observed in the P90 film after thermal annealing and this is retained after irradiation. In addition, in order to explain the modifications in the UV–vis spectra of both copolymers it is necessary to take into account changes in orientation of the chromophores with the different treatments. The band around 340–360 nm region is assigned to the transition dipole moment along the long axis of the *E*-azobenzene moiety and it is strongly affected by the molecular environment of the azobenzene as aggregation or orientation. However, the band around 250 nm due to the transition dipole moment along the short axis of the azobenzene chromophore is not influenced by both aggregation and orientation and, if the trace of the band is similar, it can be used as an internal standard in a first approximation to evaluate the orientational dependence of the π–π^* absorbance after different treatments (Table 2) [32,38]. As-prepared cast films of P50 and P90 exhibit similar $A_{\pi-\pi}/A_{\Phi-\Phi}$ values, which provide evidence of a similar spatial orientation of the chromophores. However, the significant decrease in $A_{\pi-\pi}/A_{\Phi-\Phi}$ values of P90 after annealing seems to indicate an increase of chromophores with an out-of-plane long axis component. The irradiation with *l*-CPL only produces a slightly modification of the $A_{\pi-\pi}/A_{\Phi-\Phi}$ relationship for both polymers.

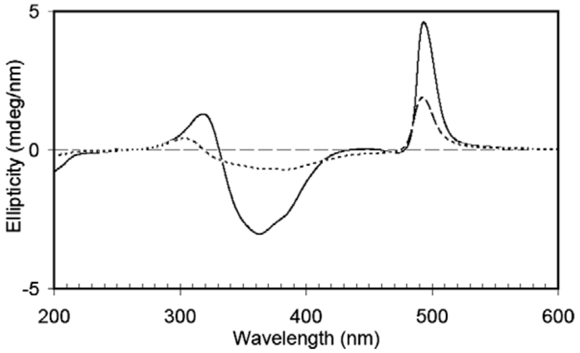

Fig. 3. CD spectra of films irradiated with *l*-CPL from the 488 nm line of an Ar$^+$ laser (20 mW/cm^2) for 30 min P50 (?) and P90 (—).

3.3. Supramolecular chirality of azobenzene units: CD study

The annealed films of P50 and P90 were irradiated with *l*-CPL from the 488 nm line of an Ar$^+$ laser (power 20 mW/cm^2) for 30 min. Both polymeric films and solutions were totally CD-silent before irradiation. However, illumination with CPL induces the appearance of a chiroptical response in the polymeric films. The CD spectra of irradiated films are shown in Fig. 3 and CD data are gathered in Table 3. In the CD spectra the ellipticity values are shown in mdeg/nm in order to compare photoinduced CD spectra of both irradiated copolymers. Furthermore, in both cases it was confirmed that the contribution of linear dichroism to the CD spectra is negligible by comparing CD spectra recorded at different angles by rotating the film around the light beam (the same region was measured in all cases).

According to the exciton model [39] two chromophores stacked with parallel transition moments exhibit an

Table 3
Main CD data[a] for thin films of the synthesized copolymers after irradiation with *l*-CPL from the 488 nm line of an Ar$^+$ laser (power 20 mW/cm^2) for 30 min.

Polymer	Wavelength (nm)			
	λ_0	λ_1	λ_2	λ_3
P50	331	318	362	492
P90	319	302	384	492

[a] λ_0, wavelength of crossover of exciton couplet; λ_1, wavelength of positive band of exciton couplet; λ_2, wavelength of negative band of exciton couplet; λ_3, wavelength of positive band corresponding to selective reflection.

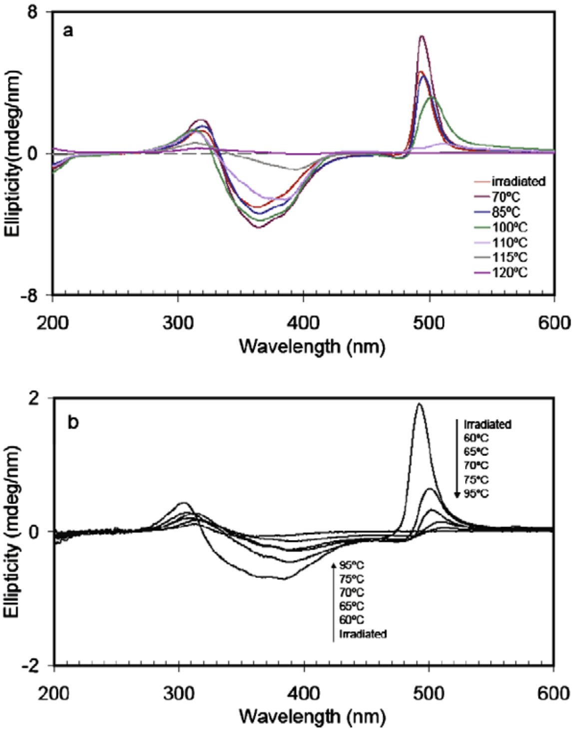

Fig. 4. CD spectra of irradiated P50 (a) and P90 (b) with *l*-CPL from the 488 nm line of an Ar^+ laser (20 mW/cm^2) for 30 min and after annealing for 5 min at the indicated temperatures.

H-band because higher energy excitation is allowed and a red-shift (J-band) is expected for the transition moments in an in-line orientation. Both of these arrangements are not chiral and consequently a CD signal should not be expected. However, two chromophores in an oblique orientation with a potential chiral array of the transition moments, both of the exciton transition (higher and lower energy), are allowed and the UV–vis band is split if the exciton splitting has sufficient energy. Thus, due to the chiral aggregation, an exciton couplet is manifested in the CD spectra as two distinct CD bands of opposite sign [39,40]. In the case of the copolymer P50 a negative exciton couplet centered at 331 nm was detected in the CD spectrum of the irradiated film. This result indicates that the *l*-CPL induces an oblique chiral arrangement between at least two azobenzene units. In addition, the negative Cotton effect at about 360 nm can include the red-shifted band of the exciton coupling and the absorption due to the induced Cotton effects of the isolated azobenzene units and the J-aggregates [27]. Finally, a positive signal was detected at around 490 nm and this can be attributed to selective reflection in the visible range because of the Bragg reflection of a helical organization similar to the selective reflection of a chiral nematic mesophase [28]. This band can be detected in the UV–vis spectrum of the *l*-CPL irradiated film (Fig. 2 Inlets). Taking into account the sign of the photoinduced selective reflection band in the CD spectra and in accordance with the optical behavior of ideal helices, the irradiation with *l*-CPL produces a left-handed helix [21]. Similar results pointed to a chiral supramolecular structure were obtained after *l*-CPL irradiation of film P90 but the intensity of the chiroptical response is clearly lower. The low intensity of the photoinduced CD band in P90 can be explained as a consequence of the out-of-plane orientation of *E*-azobenzene chromophores produced by annealing. The photoisomerization of *E*-azobenzene is only activated when the transition dipole moment of the long axis of the chromophores has a component parallel to the light polarization [7]. As a consequence, out-of-plane *E*-azobenzene chromophores are not active for the photoisomerization with CPL.

The photoinduced helixes are stable at room temperature for at least two months in the dark. The thermal stabilities of photoinduced helical organizations were studied by successively heating the irradiated films of the synthesized polymers at different temperatures for 5 min followed by quenching to room temperature in order to

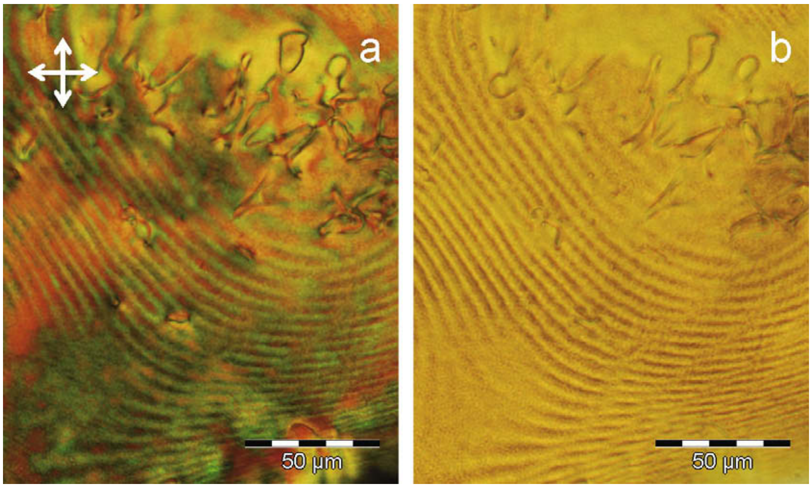

Fig. 5. Photomicrographs with crossed polarizers: optical textures of a thick film of P50 after irradiation with *l*-CPL from the 488 nm line of an Ar^+ laser (20 mW/cm^2) for 30 min with crossed polarizers (a) and parallel polarizers (b).

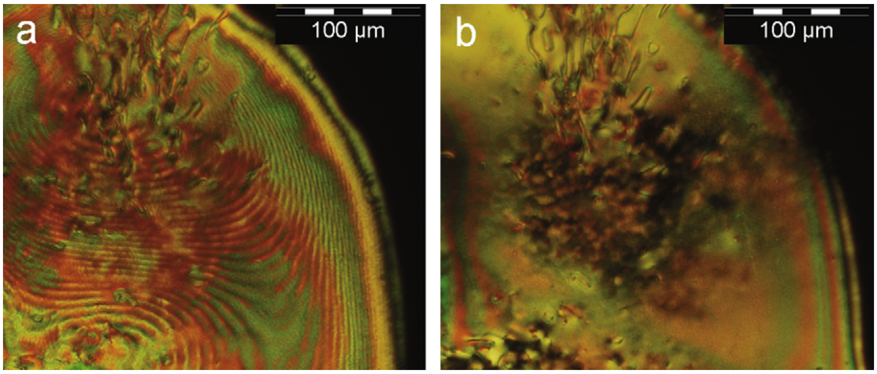

Fig. 6. Photomicrographs with crossed polarizers: optical textures of a thick film of P50 after irradiation with *l*-CPL from the 488 nm line of an Ar$^+$ laser (20 mW/cm^2) for 30 min (a) and after thermal annealing at 140 °C for 5 min at (b).

freeze-in the molecular organization [41]. The CD spectra of the films were measured after each treatment and the results are shown in Fig. 4. Thermal annealing of irradiated P50 at a temperature close to the T_g (74 °C) caused a slight increase in the ellipticity values of the CD bands corresponding to the transition band of *E*-azobenzene chromophores and the selective reflection. Annealing at temperatures above the T_g led to a gradual decrease in the ellipticity values up to 120 °C; at this temperature a significant CD signal was not detected. However, the CD artifact corresponding to selective reflection disappeared at a lower temperature (110 °C). These results could indicate that the long-range helical arrangement is destroyed at lower temperatures than the chiral aggregates. The thermal annealing of P90 led to a continuous decrease in the CD signals corresponding to the transition band and the selective reflection from 60 to 95 °C.

3.4. Optical textures

The textures exhibited at room temperature by a thick film P50 irradiated are shown in Fig. 5. Non-irradiated films exhibit an optical texture that is characteristic of the nematic mesophase but after irradiation defect lines appear. These lines are observable with and without crossed polarizers and are related to orientation of the chromophores into domains [42]. This photoinduced macroscopic structure was preserved above the T_g and up to the isotropization temperature (around 140 °C) (Fig. 6 and motion picture in Supplementary Information).

Four micrometer cells with an aligning layer for planar orientation were filled with the polymers. A photograph of a cell of P90 in which both irradiated and non-irradiated regions are observed at room temperature is shown in Fig. 7. The irradiated region exhibits a photoinduced iridescent green reflection that can be observed with the naked eye (ON, Fig. 7). This selective reflection corresponds to the photoinduced signal detected in the CD spectra at around 490 nm due to a helical supramolecular arrangement of azobenzene groups. Moreover, a significant change in the optical texture was induced by irradiation. Planar alignment was clearly present prior to illumination (Fig. 7b) and a periodic structure was generated by the CPL in the achiral liquid crystal (Fig. 7c). Similar periodic structures were photoinduced in planar alignment cells of cholesteric liquid crystals with an azobenzene dopant. These pictures are related to the strain of the cholesteric liquid crystal layers due to *E*/*Z* isomerization of the photochromic units [43]. Analogous results were obtained after irradiation of P50 in a planar cell.

4. Conclusions

The control of the non-covalent interaction of two azobenzene-containing copolymers by a chiral source

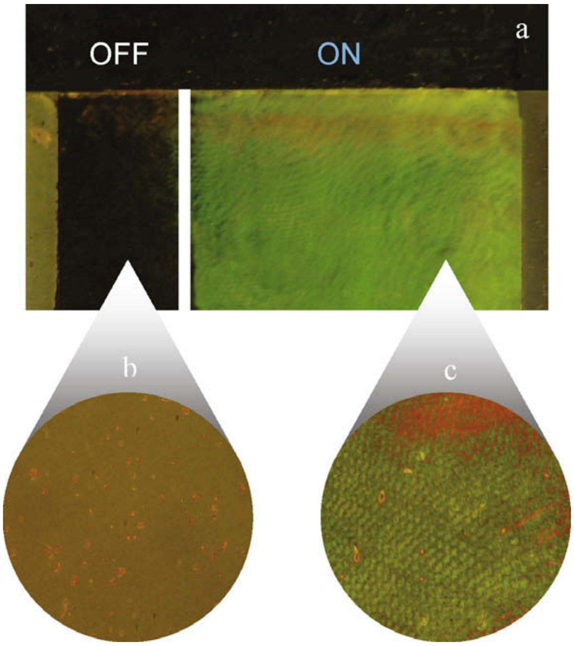

Fig. 7. P90 in a cell with an aligning layer for planar orientation: (a) Photograph taken at room temperature of photoinduced iridescent green light (irradiated zone ON); photomicrograph with crossed polarizers of the non-irradiated area (b) and irradiated area (c) of the planar cell filled with copolymer (irradiation time, 30 min; irradiation power, 20 mW/cm^2).

such as CPL provides the possibility of imprinting a chiral supramolecular organization based on the chiral aggregation of azobenzene units. Irradiation with a chiral radiation source (CPL) of nematic glasses based on achiral side-chain liquid crystalline azopolymers produces materials that are capable of selective reflection and circular polarization simultaneously as a chiral nematic glass. Moreover, the illumination with CPL of planar cells filled with the copolymers facilitates the photoinduction of a helix with axes perpendicular to the substrate, which is required in order to improve the reflectivity due to circular Bragg reflection. In addition, periodic structures are photoinduced in these planar cells. These results demonstrate the connection between light and chirality as a means of assembling complex structures in achiral photosensitive materials.

Acknowledgement

This work was supported by the Spanish MEC/MICINN projects MAT2005-06373-C02-01, MAT2008-06522-C02-01 and FEDER founding (EU).

Appendix A. Supplementary data

Supplementary data associated with this article can be found, in the online version, at doi:10.1016/j.eurpolymj.2009.05.010.

References

[1] Julian C-F. Comments on a novel approach to the role of chirality in the origin of life. Chirality 1991;3:389–92.

[2] Rau H. Chiral photochemistry. New York: Marcel Dekker; 2004.

[3] Avalos M, Babiano R, Cintas P, Jimenez JL, Palacios JC, Barron LD. Absolute asymmetric synthesis under physical fields: facts and fictions. Chem Rev 1998;98:2391–404.

[4] Hembury GA, Borovkov VV, Inoue Y. Chirality-sensing supramolecular systems. Chem Rev 2008;108:1–73.

[5] Shibaev V, Bobrovsky A, Boiko N. Photoactive liquid crystalline polymer systems with light-controllable structure and optical properties. Prog Pol Sci 2003;28:729–836.

[6] Kumar GS, Neckers DC. Photochemistry of azobenzene-containing polymers. Chem Rev 1989;89:1915–25.

[7] Natansohn A, Rochon P. Photoinduces motions in azo-containing polymers. Chem Rev 2002;102:4139–75.

[8] Matharu AS, Jeeva S, Ramanujam PS. Liquid crystals for holographic optical data storage. Chem Soc Rev 2007;36:1868–80.

[9] Halabieh RHE, Mermut O, Barrett CJ. Using light to control physical properties of polymers and surfaces with azobenzene chromophores. Pure Appl Chem 2004;76:1445–65.

[10] Dugave C, Demange L. Cis-trans isomerization of organic molecules and biomolecules: Implications and applications. Chem Rev 2003;103:2475–532.

[11] Tamaoki N, Wada M. Dynamic control of racemization rate through E-Z photoisomerization of azobenzene and subsequent partial photoresolution under circular polarized light. J Am Chem Soc 2006;128:6284–5.

[12] Choi S-W, Izumi T, Hoshino Y, Takanishi Y, Ishikawa K, Watanabe J, et al. Circular-polarization-induced enantiomeric excess in liquid crystals of an Achiral, bent-shaped mesogen. Angew Chem Int Ed 2006;45:1382–5.

[13] Vera F, Tejedor RM, Romero P, Barbera J, Ros MB, Serrano JL, et al. Light-driven supramolecular chirality in propeller-like hydrogen-bonded complexes that show columnar mesomorphism. Angew Chem Int Ed 2007;46:1873–7.

[14] Choi SW, Kawauchi S, Ha NY, Takezoe H. Photoinduced chirality in azobenzene-containing polymer systems. Phys Chem Chem Phys 2007;9:3671–81.

[15] Nikolova L, Todorov T, Ivanov M, Andruzzi F, Hvilsted S, Ramanujam PS. Photoinduced circular anisotropy in side-chain azobenzene polyesters. Opt Mater 1997;8:255–8.

[16] Nedelchev L, Matharu A, Nikolova L, Hvilsted S, Ramanujam PS. Propagation of polarized light through azobenzene polyester films. Mol Cryst Liq Cryst 2002;375:563–75.

[17] Martinez-Ponce G, Solano C, Rodriguez-Gonzalez RJ, Larios-Lopez L, Navarro-Rodriguez D, Nikolova L. All-optical switching using supramolecular chiral structures in azopolymers. J Opt A Pure Appl Opt 2008:10.

[18] Cipparrone G, Pagliusi P, Provenzano C, Shibaev VP. Reversible photoinduced chiral structure in amorphous polymer for light polarization control. Macromolecules 2008;41:5992–6.

[19] Wu YL, Natansohn A, Rochon P. Photoinduced chirality in thin films of achiral polymer liquid crystals containing azobenzene chromophores. Macromolecules 2004;37:6801–5.

[20] Iftime G, Labarthet FL, Natansohn A, Rochon P. Control of chirality of an azobenzene liquid crystalline polymer with circularly polarized light. J Am Chem Soc 2000;122:12646–50.

[21] Hore D, Wu Y, Natansohn A, Rochon P. Investigation of circular Bragg reflection in an azopolymer with photoinduced chirality. J Appl Phys 2003;94:2162–6.

[22] Kim MJ, Shin BG, Kim JJ, Kim DY. Photoinduced supramolecular chirality in amorphous azobenzene polymer films. J Am Chem Soc 2002;124:3504–5.

[23] Kim MJ, Kumar J, Kim DY. Photofabricatoin of superhelix-like patterns on azobenzene polymer films. Adv Mater 2003;15:2005–8.

[24] Pagès S, Lagugné-Labarthet F, Buffeteau T, Sourisseau C. Photoinduced linear and/or circular birefringences from light propagation through amorphous or smectic azopolymer films. Appl Phys B 2002;75:541–8.

[25] Rodriguez V, Adamietz F, Sanguinet L, Buffeteau T, Sourisseau C. Second harmonic generation Upos thermal poling and light-induced chirality in the amorphous p(DR1M) azobenzene polymer films. J Nonlinear Opt Phys 2004;13:427–31.

[26] Choi SW, Ha NY, Shiromo K, Rao NVS, Paul MK, Toyooka T, et al. Photoinduced circular anisotropy in a photochromic W-shaped-molecule-doped polymeric liquid crystal film. Phys Rev E 2006;73:021702.

[27] Tejedor RM, Millaruelo M, Oriol L, Serrano JL, Alcala R, Rodriguez FJ, et al. Photoinduced supramolecular chirality in side-chain liquid crystalline azopolymers. J Mater Chem 2006;16:1674–80.

[28] Tejedor RM, Oriol L, Serrano JL, Partal Ureña F, López González JJ. Photoinduced chiral nematic organization in an achiral glassy nematic azopolymer. Adv Func Mater 2007;17:3486–92.

[29] Shibaev VP, Plate NA. Synthesis and structure of liquid-crystalline side-chain polymers. Pure Appl Chem 1985;57:1589–602.

[30] Griffith J. Selected aspects of photochemistry. 2. Photochemistry of azobenzene and its derivatives. Chem Soc Rev 1972;1:481–93.

[31] Beveridge DL, Jaffe HH. Electronic structure and spectra of cis- and trans-azobenzene. J Am Chem Soc 1966;88:1948–53.

[32] Sapich B, Vix ABE, Rabe JP, Stumpe J, Wilbert G, Zentel R. Ordering and dewetting in spin-coated films of a liquid crystalline main chain polymer. Thin Solid Films 2006;514:165–73.

[33] Shimomura M, Ando R, Kunitake T. Orientation and spectral characteristics of the azobenzene chromophore in the ammonium bilayer assembly. Ber Bunsenges Phys Chem 1983;87:1134–43.

[34] Uchida E, Shiraku T, Ono H, Kawatsuki N. Control of thermally enhanced photoinduced reorientation of polymethacrylate films with 4-Methoxyazobenzene side groups by irradiating with 365 and 633 nm light and annealing. Macromolecules 2004;37:5282–91.

[35] Tong X, Cui L, Zhao Y. Confinement effects on photoalignment, photochemical phase transition, and thermochromic behavior of liquid crystalline azobenzene-containing diblock copolymers. Macromolecules 2004;37:3101–12.

[36] Menzel H, Weichart B, Schmidt A, Paul S, Knoll W, Stumpe J, et al. Small-angle X-ray-scattering and Ultraviolet-Visible Spectroscopy studies on the structure and structural-changes in Langmuir-Blodgett-Films of polyglutamates with azobenzene moieties tethered by alkyl spacers of different length. Langmuir 1994;10:1926–33.

[37] Freiberg S, Lagugné- Labarthet F, Rochon P, Natansohn A. Investigatoin of thermochromic in a series of side-chain, liquid crystalline, azobenzene-containing polymers. Can J Chem 2004;82(1):1–10.

[38] Sapich B, Vix ABE, Rabe JP, Stumpe J. Photoinduced self-organization and photoorientation of a LC main-chain polyester containing azobenzene moieties. Macromolecules 2005;38:10480–6.

[39] Kasha M, Rawls HR, El-Bayoumi MA. The exciton model in molecular spectroscopy. Pure Appl Chem 1965;11:371–92.

[40] Nakanishi K, Berova N. Exciton Chirality Method. Principles and Applications. In: Nakanishi K, Berova N, Woody R, editors. Exciton chirality method. Principles and applications. Deerfield Beach, Florida: VCH; 2000.

[41] Bobrovsky A, Boiko N, Shibaev V, Wendorff J. Photoinduced textturqal and optical changes in a cholesteric copolymer with azobenzene-containing side groups. Liq Cryst 2004;31:351–9.

[42] Gortz V, Goodby JW. Enantioselective segregation in achiral nematic liquid crystals. Chem Commun 2005:3262–4.

[43] Hrozhyk UA, Serak SV, Tabiryan NV, Bunning TJ. Periodic structures generated by light in chiral liquid crystals. Opt Express 2007;15:9273–80.